

# Novel Class of Organic-Inorganic Nanohybrids from Functionalized Silsesquioxane-Based Nanoparticles and Micelles of Poly(*n*-butyl acrylate)-*block*-Poly(acrylic acid)

Manuela Schumacher<sup>1</sup>, Markus Ruppel<sup>1</sup>, Markus Burkhardt<sup>1</sup>, Markus Drechsler<sup>1</sup>, Olivier Colombani<sup>2</sup>, Ralf Schweins<sup>3</sup>, and Axel H. E. Müller<sup>1</sup>

<sup>1</sup>Makromolekulare Chemie II, Universität Bayreuth, D-95440 Bayreuth, Germany. E-Mail: axel.mueller@uni-bayreuth.de

<sup>2</sup>Université du Maine, Laboratoire Polymères, Colloïdes et Interfaces, F-72095 Le Mans Cedex 09, France

<sup>3</sup>Institut Laue-Langevin (ILL), F-38042 Grenoble Cedex 9, France

## INTRODUCTION

The self-assembly of stimuli-responsive amphiphilic block copolymers has attracted great interest in academia as well as in industry due to their potential applications as drug delivery systems, nanocontainers, stabilizers of emulsion polymerizations and reagents for removal of pollutant of water. Their corresponding interpolyelectrolyte complexes (IPECs) and organic-inorganic hybrids offer the possibility to fine-tune their physico-chemical and structural properties as they may respond on external stimuli, e.g. pH, temperature, salinity. Well-defined amphiphilic diblock copolymers poly(*n*-butyl acrylate)-*block*-poly (acrylic acid) (P*n*BA<sub>x</sub>-*b*-PAA<sub>y</sub>, with *x* = 90, 100 and *y* = 100, 150, 300) has been recently shown to spontaneously self-assemble in aqueous solution under the formation of monodisperse micelles.<sup>1,2</sup>

We report the formation of a novel class of organic-inorganic nanohybrids, which are composed of these amphiphilic diblock copolymer micelles and small, water-soluble N,N-diglycidylaminopropyl silsesquioxane nanoparticles (3 nm diameter; Figure 1). Complex formation with micelles composed of P*n*BA-*b*-PAA block copolymers is attributed to specific intermolecular interactions, such as hydrogen-bonding, and ionic interactions. Indeed, Dynamic Light Scattering (DLS), cryogenic Transmission Electron Microscopy (cryo-TEM) and Small Angle Neutron Scattering (SANS) prove the formation of well-defined organic-inorganic nanohybrids. In contrast to what was reported for the interaction with linear PAA<sup>3</sup>, complex formation occurs without network or cluster formation.

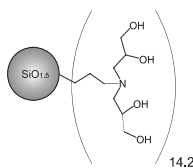


Figure 1. Structure of the silsesquioxane-based nanoparticles.

## EXPERIMENTAL

**Reagents.** The aqueous solutions were prepared using Millipore water sodium chloride, HCl (0.1M or 1M), and NaOH (0.1M or 1M). The pH was measured using a glass electrode (Methrom micro pH-electrode) connected to a Tiamo Titrande (Methrom) calibrated with three buffer solutions at pH 4.0, 7.0 and 10.0.

**Nanohybrid Formation.** Micellar solutions were obtained by dissolving the amphiphilic block copolymer in Millipore water with 1.1 equivalents of NaOH to ensure complete ionization of the PAA block. After stirring overnight, 0.1 M NaCl was added and the solutions were further stirred for 12 hours. Stock-solutions of the silsesquioxane nanoparticles (M = 3760 g/mol by MALDI-ToF-MS) were directly dissolved in Millipore water and salt was added one hour after complete dissolution. Complexes were obtained by slow addition of the stock solution of nanoparticles to the micellar solution under stirring at

pH > 9. Partial turbidity of the solution due to aggregation of larger amount of micelles with the nanoparticles vanished after seconds. The pH was adjusted by slow addition of HCl. When required, the aqueous complex solutions were dialyzed against Millipore water at same pH and salinity as the corresponding complex solutions in order to purify the aqueous hybrid solutions from excess free nanoparticles.

**Instrumentation.** DLS measurements were carried out at scattering angles ranging from 30 to 150° with an ALV DLS/SLS-SP 5022F equipment consisting of an ALV-SP 125 laser goniometer, a ALV 5000/E correlator processing in cross-correlation mode, and a He-Ne laser ( $\lambda = 632.8$  nm). The CONTIN algorithm was applied to analyze the obtained autocorrelation functions.

Cryo-TEM measurements were performed on a Zeiss EM922 EF-TEM with an acceleration voltage of 200kV. The sample preparation procedure was performed as described elsewhere<sup>2</sup>.

Samples for SANS were prepared in D<sub>2</sub>O. Measurements were performed using the instrument D11 at ILL (Grenoble, France) with a neutron wavelength of 6 Å (corresponding to a scattering vector *q* of 0.003 – 0.34 Å<sup>-1</sup>) with sample-to-detector distances of 1.1, 4 and 16 m in 1 or 2 mm quartz cells at room temperature. The SANS curves still contain the incoherent background scattering of the solvent and the sample.

## RESULTS

DLS measurements reveal the particles size distribution for an increasing content of nanoparticle in the micellar solution (Figure 2). Evidently, only unimodal distributions with low dispersity are observed even for a large excess of nanoparticles in solution. This clearly indicates the absence of cluster formation even at very high concentrations of the silsesquioxane-based nanoparticles (Figure 2).

Table 1. Comparison of the Pure Micelles and the Organic-Inorganic Nanohybrids at pH > 9 and 0.1 M NaCl

P <i>n</i> BA <sub>x</sub> - <i>b</i> -PAA <sub>y</sub>		Pure Micelles <sup>2</sup>				Hybrids
		R <sub>h,DLS</sub> [nm]	R <sub>c,SANS</sub> [nm] <sup>a</sup>	N <sub>agg</sub> <sup>b</sup>	N <sub>COOH</sub> <sup>c</sup>	
x	y					R <sub>h,DLS</sub> [nm]
90	300	52	9.7	270	81,000	54
100	150	52	9.7	370	56,000	57
90	100	29	11.3	440	44,000	33

<sup>a</sup>core radius according to SANS; <sup>b</sup>aggregation number; <sup>c</sup>number of acid functions per micelle

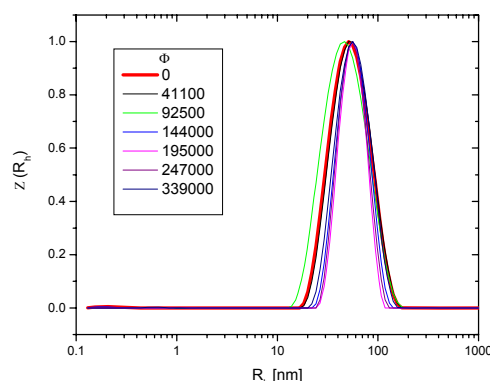
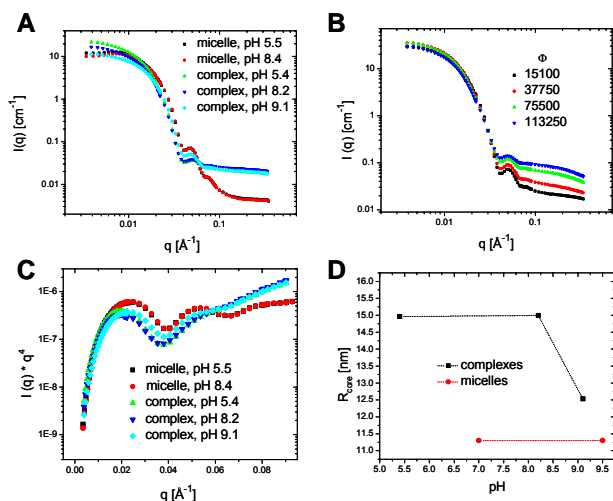


Figure 2. Intensity weighted CONTIN plot of complexes prepared of P*n*BA<sub>90</sub>-*b*-PAA<sub>300</sub> with varying amount of silsesquioxane-based nanoparticles at pH > 9 and 0.1 M NaCl at 90° scattering angle [ $\Phi = n(\text{nanoparticle})/n(\text{micelle})$ ;  $\Phi = 0$  corresponds to the pure micelle].

As seen from Table 1, the sizes of the hybrid particles are only slightly larger than those of the pure micelles. This may be assigned to the presence of neutralizing effects upon complex formation: the shrinkage of the micelles upon screening of the negatively charged corona by the positively charged nanoparticles on the one hand and the expansion of the corona owing to the high osmotic pressure of the entrapped nanoparticles together with sterical constraints on the other hand. It is noteworthy that even at a high molar excess of the nanoparticles they do not contribute to the autocorrelation function and

therefore were not evident in the corresponding particle size distribution. Whereas this may be attributed to the complex formation in the presence of nanoparticles, this may be misleading at very high nanoparticle concentrations where free nanoparticles would be expected. The free nanoparticles are not detected even for a very high excess of nanoparticles. This is assigned to their small size ( $R_h = 1.5$  nm) compared to the micelles, which therefore exclusively contribute to the intensity-weighted autocorrelation function even at high nanoparticle concentrations.

SANS measurements also sustain the formation of well-defined organic-inorganic nanohybrids (Figures 3A,B). With an increasing nanoparticle content,  $\Phi = n(\text{nanoparticle})/n(\text{micelle})$ , entrapped within the micelles the characteristic oscillations for spherical particles become less pronounced (Figure 3B).



**Figure 3.** SANS curves of  $PnBA_{90}$ - $b$ - $PAA_{100}$  and the corresponding complexes (A) after dialysis at varying pH values and with increasing content of nanoparticles without dialysis at pH 10 (B) with 0.1 M NaCl. (C) Porod plot of pure  $PnBA_{90}$ - $b$ - $PAA_{100}$  and the dialyzed complexes at different pH values. D shows the core radii of the pure micelles and the corresponding dialyzed complexes according to a Guinier fit.

Furthermore, the Porod representation of the scattering data of the complexes illustrates a shift of the first maxima to lower  $q$  values compared to the corresponding maxima of the pure micelles (Figure 3C). This strongly indicates an increasing apparent core radius of the nanohybrids. This is confirmed by a Guinier evaluation of the scattering data (Figure 3D). The core radii significantly increase from 11 nm for the pure micelles up to 12 to 15 nm in case of the dialyzed nanohybrids. SANS measurements at different pH of the dialyzed saline nanohybrid solutions indicate a decreasing apparent core radius at  $pH > 8.5$ , which is assigned to a release of entrapped nanoparticles at high pH in thermodynamic equilibrium.

Cryo-TEM micrographs confirm the formation of well-defined nanohybrids (Figure 4). They clearly show the presence of single particles in aqueous solution without the formation of micellar networks or clusters. Note that micellar corona is only partially visible even when stained with CsOH. (Fig. 4A,C) as the contrast of the stretched PAA arms is not so distinct compared to the background (water). The averaged radially integrated gray-scale intensity shows a sharp increase of the gray value close to a radius of 10 nm demonstrating the sharp interface between core and corona. This is well in agreement with the core radii determined by SANS experiments.

In the corresponding cryo-TEM micrographs of the nanohybrids the situation is remarkably different. Obviously, the transition at the core-corona interface is less pronounced and ill-defined (Fig. 4B). Three different regions may be distinguished according to the gray scale analysis (Fig. 4D): The first transition is evident at  $r \sim 10$  nm. Again this is easily assigned to the core-shell vicinity. The second region ( $r \sim 10$ – $21$  nm) may be assigned to a dense packing of nanoparticles in the inner part of the corona close to the core-corona

interface. Here, the degree of packing is obviously decreasing. At distances  $r > 21$  nm the gray scale analysis clearly demonstrates a significant higher mass contrast compared to the pure micelles, which is gradually decreasing. This is interpreted in terms of entrapped nanoparticles that are less congestedly distributed within the outer part of the corona, exhibiting a radial density gradient. This is indicative of a core-shell corona morphology of the nanohybrids, which may be directly visible in the corresponding cryo-TEM micrographs.

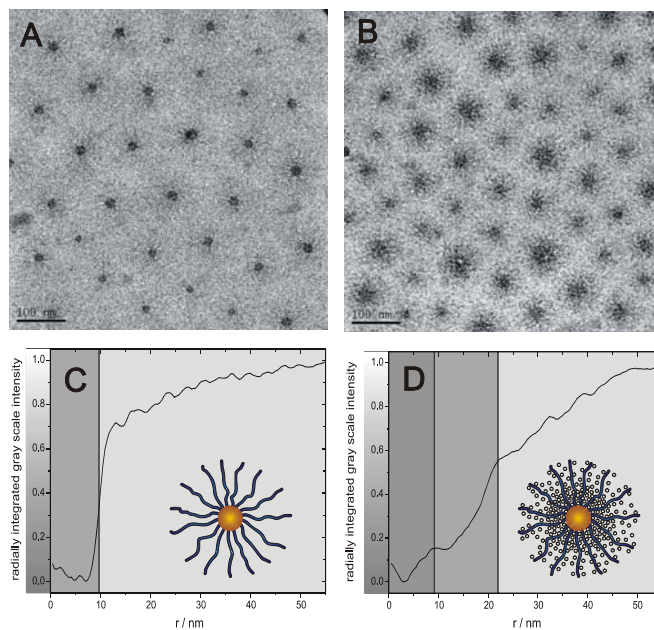


**Figure 4.** Cryo-TEM micrographs of  $PnBA_{90}$ - $b$ - $PAA_{300}$  micelles (5 g/L) (A) and complexes (B) at pH 7, stained with CsOH. The complexes are prepared as mass equivalents of nanoparticles and the amphiphilic diblock copolymer. The averaged radially integrated gray-scale intensity of the pure micelle (C) and the complexes (D) are shown.

## CONCLUSION

The experimental data clearly demonstrate the formation of novel well-defined organic-inorganic nanohybrids in aqueous solution consisting of  $PnBA$ - $b$ - $PAA$  block copolymer micelles and highly functionalized silsesquioxane-based nanoparticles. These nanohybrids do not undergo network or cluster formation in saline solution at  $pH > 7$  even in the presence of a molar excess of nanoparticles. Cryo-TEM micrographs strongly indicate a core-shell corona morphology of this novel class of water-soluble self-assembled supramolecular hybrid structures.

## ACKNOWLEDGEMENTS

This work was supported by DFG. The authors thank A. Walther for his help with the SANS experiments. J. E. Klee (Dentsply DeTrey, Konstanz), G. Ch. Behera and K. Möller are gratefully acknowledged for the preparation of the silsesquioxane-based nanoparticles.

## REFERENCES

- Colombani, O.; Ruppel, M.; Schubert, F.; Zettl, H.; Pergushov, D. V.; Müller, A. H. E. *Macromolecules*, submitted.
- Colombani, O.; Ruppel, M.; Burkhardt, M.; Drechsler, M.; Schumacher, M.; Gradzielski, M.; Schweins, R.; Müller, A. H. E. *Macromolecules*, submitted.
- Mori, H.; Lanzendörfer, M. G.; Müller, A. H. E.; Klee, J. E. *Macromolecules* **2004**, *37*, (14), 5228-5238.